Phys Chem Minerals (2003) 30: 125–130
DOI 10.1007/s00269-003-0297-3

ORIGINAL PAPER

S. Heinemann · R. Wirth · G. Dresen

TEM study of a special grain boundary in a synthetic K-feldspar bicrystal: Manebach Twin

Received: 13 February 2002 / Accepted: 24 December 2002

Abstract A monoclinic $KAlSi_3O_8$ feldspar Manebach twin boundary was synthesized by diffusion bonding and examined using high-resolution transmission electron microscopy. The sharp (001) twin boundary is straight and free of strain. The boundary width is smaller than d_{001}. There is no rigid body shift observed at the twin boundary, and the feldspar structure is arranged symmetrically across (001). The twin boundary structure consists of bridged tetrahedral crankshafts, which are characteristic of the feldspar lattice. The grain boundary structure is in good agreement with the geometrical model of Taylor et al. (1934). The grain boundary composition of $K_{1/2}H_{1/2}AlSi_3O_8$ differs from their model.

Keywords Grain boundary structure · K-feldspar · Twins · Diffusion bonding

Introduction

Feldspars are aluminosilicates with monoclinic or triclinic crystal symmetry. The structure is composed of corner-sharing AlO_4 and SiO_4 tetrahedra forming an infinite three-dimensional array (Smith 1988). In feldspars, exsolution lamellae (special oriented phase boundaries between different feldspars) and twin boundaries (special oriented grain boundaries between identical feldspars) are common (Smith 1988). Irrespective of their low symmetry, feldspar minerals display a large variety of twins. For monoclinic and triclinic crystals 11 and 19 twin types are known, respectively. This does not include merohedral and antiphase twins. The geometry and the macroscopic grain-boundary parameters of the twin boundaries are known (Smith 1988). However, the microscopic grain-boundary parameters are unknown and structural models exist for only a few twin types.

S. Heinemann (✉) · R. Wirth · G. Dresen
GeoForschungsZentrum Potsdam,
Telegrafenberg D426, 14473 Potsdam, Germany
Tel.: + 49-(0)331–288 1323
Fax: + 49-(0)331–288 1328
e-mail: stefan.heinemann@gfz-potsdam.de

Twin boundaries in feldspar

Two different types of twins occur that are related to the monoclinic/triclinic phase transition, or to crystal growth, respectively. The former type depends on the structure and properties of the feldspar crystal structure. The latter is related to the grain-boundary structure, that differs from the bulk crystal structure in coordination numbers, topology and connectivity of the atoms.

In alkali feldspars, Si/Al ordering or a displacive mechanism causes a phase transition from monoclinic to triclinic symmetry. The monoclinic structure is characterized by two distinct tetrahedral sites (T1 and T2) but in the triclinic structure there are four distinct sites (T10, T1m, T20, T2m) (Smith 1988). The phase transition is ferroelastic (Salje 1990), producing albite twins and pericline twins. High-resolution transmission electron microscopy (HRTEM) studies indicate that albite and pericline twin walls are diffuse (Salje 1990). The width of pericline twin walls in anorthoclase feldspar is 2.5 nm at 300 K and 12 nm at 700 K (Hayward et al. 1996); it increases with increasing temperature up to the phase transition. The structure of the ferroelastic twin walls consists of triclinic and monoclinic versions of the feldspar crystal structure. The symmetry in the twin wall changes gradually from triclinic in the adjacent crystals to monoclinic in the twin boundary core. Coordination number, topology and connectivity of the atoms remain similar to the undisturbed lattice, but bond length and bond angles are modified and the crystal lattice is strained across the twin boundary. The twin boundary width, the grain-boundary mobility, the ferroelastic deformation properties, its diffusivity and segregation have been investigated (Salje 1990, 1995; Hayward et al. 1996), and all these twin boundary properties are related

to the triclinic and monoclinic crystal structures of feldspar and their crystal properties.

The second most prominent type of twins in feldspar is growth twins. Primary twins form by continuous growth of a single crystal. Secondary twins may develop by crystal growth on an exposed plane of a seed crystal (Zorz et al. 1998). Oriented attachment of two crystals is another possible mechanism for growth twinning (Penn and Banfield 1998). Direct bonding (Heinemann et al. 2001) of two $KAlSi_3O_8$ feldspar single crystals was recently achieved.

Growth twin boundaries are sharp in contrast to ferroelastic twin walls (Sutton and Baluffi 1995). Their width is approximately one or two unit cells (Wolf and Yip 1992). The structure of a sharp grain boundary is significantly different from the regular crystal lattice, as the average coordination number of atoms is reduced and the average bond length is changed. This requires elastic and plastic relaxation of the crystal lattice along the grain boundary on the atomic scale and compensation of resulting electric charges. The structural rearrangement commonly produces an excess free volume at the boundary. The difference between grain-boundary structure and the crystal lattice and required charge compensation will affect the grain-boundary physical and chemical properties. In general, non-special oriented grain boundaries are as sharp as growth twin boundaries.

The physical and chemical properties of diffuse and sharp grain boundaries are fundamentally different (Sutton and Baluffi 1995), the former reflecting the attributes of the crystal structure and the latter those of the grain-boundary structure. Therefore, the results from well-investigated ferroelastic boundaries cannot be applied to general grain boundaries and their properties. However, feldspar growth twin boundaries are mostly sharp, similarly to most grain boundaries. Symmetric grain boundaries may be regarded as fixed points in the grain-boundary structure continuum similarly to crystal structures of the pure end members in a solid-solution series.

For feldspar growth twins, geometry was determined using only macroscopic methods (Smith 1988). Grain-boundary parameters, like orientation of the grain-boundary plane, rotation axis and rotation angle, are known. However, microscopic parameters, like rigid body shifts in the grain-boundary plane which are smaller than the length of a unit cell, and the grain boundary structure are unknown. The structures of the Carlsbad, Baveno and Manebach twins were postulated using structural arguments (Smith 1988). However, HRTEM images exist only for Carlsbad twins (Xu et al. 1997) and were not interpreted. Two different models are proposed for Manebach twins, which differ in microscopic parameters (Taylor et al. 1934; Wooster 1981).

Natural grain boundaries are interfaces containing defects like voids, mineral and fluid inclusions, pores, impurities, stacking faults, dislocations and point defects (White and White 1981; Bons et al. 1990; Elbert and Veblen 1997; Hiraga et al. 1999). Tailoring synthetic grain or twin boundaries containing a minimum number of defects allows studying the structural and transport properties of natural grain and phase boundaries (Heinemann et al. 2001).

In this paper we investigate the structure of a synthetic twin boundary using high-resolution transmission electron microscopy (HRTEM). The observations allow the discrimination and improvement of existing structural models (Taylor et al. 1934; Wooster 1981).

Experimental

Starting material

The starting material was a gem-quality monoclinic potassium feldspar crystal with yellowish colour from Itrongay, Madagascar (Gebrüder Bank, Idar-Oberstein, Germany). Since the first description by Lacroix (1912), the potassium feldspar gems from Madagascar have been called orthoclase; they are, however, low sanidines (Priess 1981). The crystal is free of twins, exsolution lamellae and inclusions. Microprobe analysis shows only minor concentrations of iron and sodium: $K_{0.928(8)}Na_{0.053(2)}Al_{0.946(15)}Fe_{0.049(14)}Si_{3.021(5)}O_{8.024(7)}$. The lattice parameters were determined by powder X-ray diffraction in transmission mode: $a = 0.8584(1)$ nm, $b = 1.3006(3)$ nm, $c = 0.7190(1)$ nm, ß = 116.016(7) °. The crystal is monoclinic because the characteristic (131) reflection shows no splitting, and therefore the space group is $C2/m$.

Potassium feldspar single crystal plates (10 x 10 x 1 mm) were oriented with X-ray diffraction parallel to (001). The (001) faces of the square plates were chemo-mechanically polished with silica slurry (pH = 11) (CRYSTAL, Berlin). The final average roughness (deviation from a mean surface line) of the crystal plates was 0.139 nm. The roughness was measured without contacting the surface using interferometry (Kugler KMS microscope).

Synthesis

The synthetic Manebach twin boundary investigated in this study was produced by diffusion bonding under high vacuum. For diffusion bonding a uniaxial load is applied perpendicular to the interface contact of two crystals (Derby and Wallach 1982; Hill and Wallach 1989; Orhan et al. 1999). Stresses are typically some small fraction of the room-temperature yield stress, for example 1 MPa for Mo or Ta (Campbell et al. 1999, 2000), 5 MPa for YAG (Campbell 1996) and 0.5–3 MPa for $SrTiO_3$ (Hutt et al. 2000). Temperatures required for diffusion bonding are in the range of 50–80% of the absolute melting point of the material. The macroscopic grain-boundary parameters can be controlled by selecting the grain-boundary plane and the crystal orientation angle. However, the microscopic grain-boundary parameters, namely the rigid body shifts below the crystal periodicity within and perpendicular to the grain-boundary plane, are self-organized, and the microscopic grain-boundary structure is the result of a bonding experiment.

The sample was heated by induction of an Mo recipient, and temperature was controlled by a PtRh30–PtRh6 thermocouple. A maximum load of 1.4 MPa perpendicular to the interface was applied at high temperature. The vacuum pump started 14 h before the heating, and after ca. 10 h 95% of the final vacuum was established. The vacuum at room temperature was 4.46×10^{-4} Pa and increased to 6.7×10^{-4} Pa at 400 °C. Temperature was increased to 934 °C within 2 h. The sample was annealed for 2 h, and then cooled to room temperature with maximum cooling rate of 7.25 °Cmin^{-1}. After cooling, the vacuum and the load were released. Finally, the bicrystal was annealed at 1060 °C for up to 4 weeks and slowly cooled (5 °Cmin^{-1}) to ambient temperature.

Chemical composition of the boundary region was determined using energy dispersive X-ray analysis in TEM of scanned areas of 50 nm width perpendicular to the grain boundary. The area composition at the grain-boundary region is identical with the areas at neighbouring crystals.

Specimen preparation and TEM

The bicrystal was cut parallel to the interface and glued into a slit of an Al_2O_3 ceramic specimen holder (Strecker et al. 1993). Subsequently, slices were cut from this assembly and dimpled (GATAN) from both sides to a thickness of 15 μm. Finally, the specimens were ion-milled (GATAN Duomill; 5 kV, 11 °) and carbon-coated.

HRTEM was performed in a Philips CM200 microscope equipped with an LaB_6 filament as electron source and a GATAN imaging filter (GIF). The sensitivity of the specimen to electron irradiation damage was overcome by using the CCD camera of the GIF, which allowed exposure times of only 1–2 s. The HRTEM images are energy-filtered by applying a 10-eV slit to the zero loss peak. The chemical composition was measured using an EDAX X-ray analyzer with ultrathin window.

Results

Figure 1a shows a cross section of the grain boundary in high resolution and edge on. The bicrystal halves are above and below the grain boundary. Their zone axes are [010] and [0$\bar{1}$0], respectively. The area of the marked box around the grain boundary was filtered (fast Fourier filtered, FFT) and is shown in Fig. 1b. The cross-section of the grain boundary in the centre of the image is running E–W. The projections of the prominent (100), (001) and (201) lattice planes are perpendicular to the image plane and parallel to the viewing direction. (100) and (001) lattice fringes are indicated. The twin boundary plane is (001), as indicated. It is straight and shows no strain contrasts. For the bicrystal halves, the **a** direction of the lattice is oriented parallel to the trace of the boundary. The (100) planes of both crystals are inclined to the interface. They meet at the twin boundary plane and the boundary is coherent and sharp. The grain-boundary structure is periodic and no amorphous layer is observed at the boundary. The d_{001} lattice fringe spacing parallel to the grain boundary remains constant near the grain boundary. The structural grain-boundary width is smaller than one crystal structure unit cell, hence smaller than d_{001}. The chemical composition is equal to the neighbouring bicrystal halves in an interval of 50 nm perpendicular to the grain boundary. The feldspar structure beyond the grain boundary is symmetrically arranged with respect to the grain-boundary plane. The unit cells of the feldspar structures are marked in the upper and the lower half of the twin. The (100) lattice fringes meet symmetrically at the grain-boundary plane without a rigid body shift in the **a** direction. The microscopic twinning agrees with the macroscopically determined twin law (Smith 1988). However, a shift of **a**/2 between the upper and lower lattice rows is still possible.

Fig. 1 **a** Energy-filtered HRTEM image of synthesized K-feldspar interface (interface perpendicular to the image) of zone [010]. The area shows no defects and no strain along the coherent twin boundary. The trace of the boundary is parallel to the a direction. *Inserted box* marks the area of **b**. **b** Fourier-filtered (FFT) image of the interface of the box in **a**. The twin boundary is horizontal at the *centre of the image*. The *c* directions of the upper and lower halves meet at the twin boundary. **c** Geometrical structure model for the twin boundary of Taylor et al. (1934) (Fig. 3a). Oxygens are not shown. The model agrees with HRTEM in **b**

Discussion

Crystal structure of K-feldspar

The structure of $KAlSi_3O_8$ feldspar consists of rings of four corner-linked $(Al,Si)O_4$ tetrahedra (Fig. 2a). The rings contain alternating T1 and T2 tetrahedral positions with alternating T1–O–T2 and T2–O–T1 bridges. In disordered monoclinic $KAlSi_3O_8$, the Al/Si distributions at the eight tetrahedral positions T1 and eight T2 per unit cell are equal: 6Si + 2Al. In ordered monoclinic $KAlSi_3O_8$ aluminium is present only at T1, whereas the T2 are occupied by silicon only; T1: 4Si + 4Al; T2: 8Si. The tetrahedra rings are arranged horizontally and vertically in regard to the (010) plane. The horizontal tetrahedra rings contain a twofold [010] axis in their centre and the vertical rings contain a twofold screw [010] axis at their centre. Horizontal and vertical rings share two common tetrahedra, as arrangement similar to a crankshaft parallel to the **a**-direction. T1, T2 tetrahe-

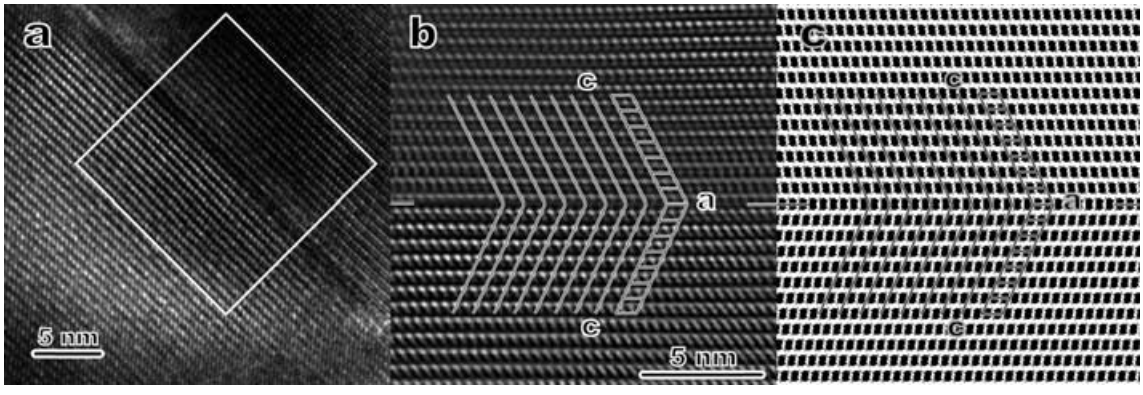

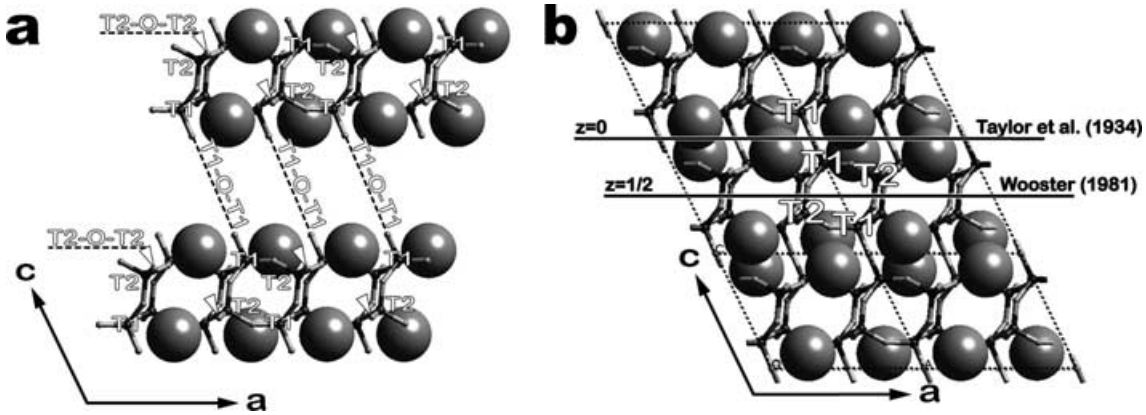

Fig. 2a,b Structure of monoclinic $KAlSi_3O_8$ feldspar with tetrahedral Al/Si disorder viewed along [010]. Oxygen anions are shown in reduced size. **a** Crankshafts of horizontal and vertical four-rings of tetrahedra. T1 and T2 tetrahedral positions alternate in the rings and in the crankshafts. The crankshafts are connected by equal tetrahedra: T1–O–T1 bridges across the plane (001) (*dashed lines*) and T2–O–T2 bridges across the image plane (010) (*arrows*). Potassium cations are between the crankshafts. **b** Complete structure shows large channels of horizontal tetrahedra rings at $z = 1/2$ and small channels of four potassium cations and two tetrahedra at $z = 0$. The Manebach twin boundary (001) is located at $z = 0$ in the model of Taylor et al. (1934) and at $z = 1/2$ in the model of Wooster (1981)

dral types and T1–O–T2, T2–O–T1 bridges alternate in the crankshafts and in the rings. Two crankshafts are contained in one unit cell (Fig. 2b). In monoclinic feldspars ($C\ 2/m$) the crankshafts are symmetrically transformed by the mirror planes (010) between them at y = 0 and y = 1/2. The crankshafts are corner-linked by equal tetrahedra types: T1–O–T1 tetrahedra bridges with the bridging oxygen at the twofold axes x = 0,1/2 in the (001) planes at $z = 0$ and T2–O–T2 tetrahedra bridges at the mirror planes at y = 0,1/2. Between the crankshafts the potassium cations are arranged in nine-fold polyhedral cages at the mirror planes.

Structural models of the Manebach twin

The macroscopic Manebach twin law in feldspar is a 180° rotation about the normal of the plane (001). A mirror reflection at the plane (001) is equivalent because feldspar is centrosymmetric. The twin law was determined by polarized light and X-ray methods (Smith 1988). The optimal twin boundary of the Manebach twin is (001) (Pellegrini 1971). Two different microscopic models were developed based on twin geometry and feldspar structure (Taylor et al. 1934; Wooster 1981). The models show a symmetric microscopic arrangement of the tetrahedra and the feldspar structure in accordance with the macroscopically determined twin law. No rigid body translation parallel to the twin boundary occurs in the models, but different positions of the composition plane (001) are predicted in a direction parallel to the *c* axis. Relaxation of the structures into an exact twin boundary configuration is not included in the models.

Taylor et al. (1934) suggested that the composition plane (001) is located at $z = 0$, where the crankshafts of the feldspar structure are connected via bridged T1–O–T1 tetrahedra across the *c* plane (Fig. 2b). The application of the twin law juxtaposes planes with intact crankshafts, rings and tetraheda, and the twin individuals are recombined by linked T1–O–T1 tetrahedra (Fig. 3a). The K–O polyhedra are cut by the composition plane (001) into parts with and without the potassium cations. The construction of this twin boundary model from the twin individuals and the application of the twin law creates overlapping potassium cations at the composition plane. The strain of the neighbouring lattice is minimized.

In contrast, Wooster (1981) postulated that the composition plane (001) cuts the crankshafts and their tetrahedra rings at $z = 1/2$ (Fig. 2b). The composition plane contains no atoms, but cuts the tetrahedral T1–O–T2 bonds of the linked tetrahedra. After the application of the twin law the twin individuals connect through deformed tetrahedra which are bridged as T1–O–T1 and T2–O–T2. However, the geometrical construction reveals that a tetrahedral connection is only possible if the tetrahedra are strained. This can be achieved by tilting or shortening the connected tetraheda or by elongating the bond length of the disconnected tetrahedra, and new fourfold tetrahedra rings are formed.

In addition, a twin model with the composition plane (001) at $z = 1/2$ can be constructed if the twinned crystal parts are shifted asymmetrically along the **a** direction with respect to each other till the twin individual are connected by the bridged tetrahedra T1–O–T2 and T2–O–T1. The rigid body shift is smaller than **a**/2 and the bicrystal parts are asymmetrically arranged. This microscopic rigid body translation in the **a**-direction violates the macroscopic twin law but would remain undetected in polarized light microscopy or X-ray diffraction.

We found no other possible tetrahedral T–O–T connection to recombine crystal segments that were previously separated at $z = 0$ or $z = 1/2$. Since tetrahe-

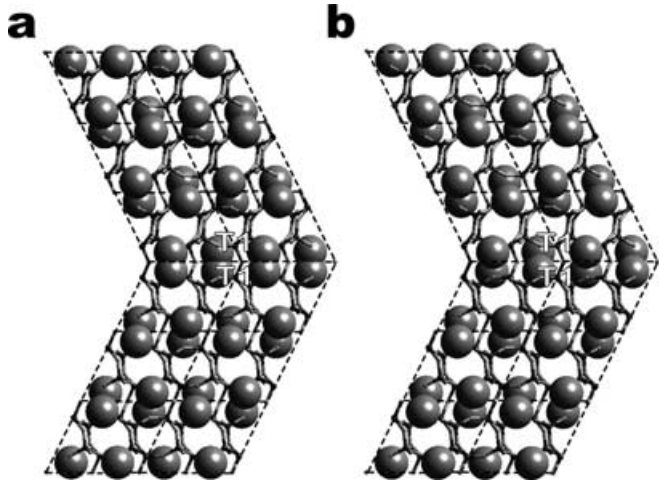

Fig. 3 **a** Symmetric Manebach model of Taylor et al. (1934) with the twin boundary at $z = 0$. Crankshafts are linked at the grain boundary plane by T1–O–T1 bridges. Potassium cations overlap in pairs at the grain boundary. **b** Manebach model with composition $K_{1/2}H_{1/2}AlSi_3O_8$ at the grain boundary. Hydrogen is located as bridging hydroxyl T–OH–T in statistical disorder around the empty cation position

dral T–O–T linkage is the main building principle in the feldspar framework, we exclude all models without it. We conclude that the two symmetric models and the asymmetric model are the only configurations possible for the Manebach twin boundary.

HRTEM observations

The HRTEM observations show a symmetric arrangement at the twin boundary without rigid body shift. For this reason, the asymmetric twin model with the T1–O–T2 tetrahedral connection is excluded. However, a shift of **a**/2 between the upper and lower crystal lattice is still possible. In the case of the composition plane at $z = 0$ and $z = 1/2$ all bridging tetrahedra are disconnected and have their dangling T–O bonds at maximum distance to each other. The feldspar framework cannot be bridged across the twin boundary. This possibility is unreasonable and has been already excluded in the search for possible twin-boundary models.

The spacing of the (001) lattice planes parallel to the grain boundary does not change across and in the vicinity of the twin-boundary plane. This information is used for the geometric grain-boundary models of Taylor et al. (1934) and Wooster (1981). A comparison of the HRTEM images with the structural models shows a very good agreement with the Taylor model. The indicated unit cells of the feldspar structure suggest that the (001) twin boundary is at the position $z = 0$, but not at $z = 1/2$, as expected from the Wooster model. The Wooster model requires the twin boundary to be located at $z = 1/2$, but this is not observed in TEM. We found no indication of lattice strain, as necessary for the model of Wooster (1981).

Deviation from Taylor's Manebach model

The Manebach model of Taylor et al. (1934) explains well the tetrahedral framework structure at the grain boundary, but the overlapping of potassium cations in pairs at the grain-boundary plane seems to be an argument against this model. In principle, the construction of their model is the cleavage of feldspar at the plane (001) in the height $z = 0$, the application of the twin law and the joining of the two crystal parts at their exposed surfaces. However, cleaved feldspar surfaces contain broken dangling bonds which react immediately with air (Nyfeler et al. 1997) and preferentially with water, due to the hydrophilic surface character. The initial state of the feldspar surfaces prior to diffusion bonding can be derived from the surface structure determination of Fenter et al. (2000), who showed that Madagascar orthoclase feldspar from Itrongay does, in fact, cleaves indeed at $z = 0$ along (001). In contact with water, the (001) surface structure is the structure of $KAlSi_3O_8$ feldspar with $HAlSi_3O_8$ feldspar at the outermost cation layer, which terminates with dangling non-bridging T1–OH silanol groups (Si–OH) and aluminol groups (Al–OH). In $HAlSi_3O_8$ feldspar, hydrogen is present as bridging hydroxyl T–OH–T in a statistical disorder around the empty cation place (Paulus and Müller 1988). Similar feldspar surface structure was found by Teng et al. (2001) over a broad pH range. Consequently, we expect that replacement of potassium cations by protons occurred near the sample surface during preparation in a hydrous environment. This suggests that the formation of a Manebach twin by recombination of two crystals may not create steric problems related to the juxtaposition of two potassium ions. The bonding of the two crystals is the polymerization reaction of the dangling-surface silanol and aluminol groups to silicate bonds across the interface at ~150 °C (Heinemann et al. 2001):

$$\text{T1–OH} + \text{OH–T1} \rightarrow \text{T1–O–T1} + H_2O.$$

Presumably, dehydration of water from the interface region occurs during heating of the samples in vacuum.

The two hydrogen layers at the interface can be exchanged with potassium from the crystal by diffusion to a maximum of half the hydrogens and the composition at the interface is $K_{1/2}H_{1/2}AlSi_3O_8$ (Fig. 3b). This Manebach interface structure is in the projection along *b* identical to the model of Taylor et al. (1934) because the potassium cations are in a row and projected onto the image plane (Fig. 3). In our experiment, the surfaces where not cleaved but polished to the average surface roughness of 0.139 nm (d_{001} of unit cell ca. 0.65 nnm) and the height of asperities is reduced during the bonding procedure by diffusion at high temperatures. The surface position *z* was not controlled; nevertheless, the crankshaft structure state is rebuilt. The preference of the crankshafts suggests a domination of this structural unit at interfaces. In the case of the Carlsbad twin with the interface at the cleavage plane (010),

crankshafts should be present and joined by tetrahedral T2–O–T2 bridges.

In nature, Manebach twins often occur as contact twins. They may form from secondary crystallization of the twin individual at an exposed (001) cleavage plane (e.g., Zorz et al. 1998). Under natural conditions, water is always present and the surface structure of Fenter et al. (2000) is expected in this case. Dissolution at the (001) plane occurs stochiometrically in unit-cell layers and the surface structure is reproduced (Teng et al. 2001). The secondary crystallization of $KAlSi_3O_8$ on top of the surface structure of Fenter et al. (2000) may not create steric problems related to the juxtaposition of two potassium ions. The immediate grain-boundary composition at the secondary crystallization is $K_{1/2}H_{1/2}AlSi_3O_8$ and will result in the same interface structure as received by the synthesis of attached crystals.

Acknowledgements We thank M. Rühle, S. Hutt, J. Mayer, A. Strecker and U. Salzberger at MPI, Stuttgart, for their support and valuable advice in preparing TEM sections of bicrystals.

References

Bons AJ, Drury MR, Schryvers D, Zwart HJ (1990) The nature of grain boundaries in slates. Phys Chem Miner 17: 402–408

Campbell GH (1996) Σ5 (210)/[001] Symmetric tilt grain boundary in yttrium aluminium garnet. J Am Ceram Soc 79: 2883–2891

Campbell GH, Belak J, Moriarty JA (1999) Atomic structure of the Σ5 (310)/[001] symmetric tilt grain boundary in molybdenum. Acta Mater 47: 3977–3985

Campbell GH, Belak J, Moriarty JA (2000) Atomic structure of the Σ5 (310)/[001] symmetric tilt grain boundary in tantalum. Scripta Mater 43: 659–664

Derby B, Wallach ER (1982) Theoretical model for diffusion bonding. Metal Sci 1: 49–56

Elbert DC, Veblen DR (1997) HRTEM observations of grain boundaries and nanopores in crystalline rocks. Geol Soc Am 29: 460

Fenter P, Teng HH, Geissbühler P, Hanchar JM, Nagy KL, Sturchio NC (2000) Atomic-scale structure of the orthoclase (001)–water interface measured with high-resolution X-ray reflectivity. Geochim Cosmochim Acta 64: 3663–3673

Hayward SA, Chrosch J, Salje EKH, Carpenter MA (1996) Thickness of pericline twin walls in anorthoclase; an X-ray diffraction study. Eur J Mineral 8: 1301–1310

Heinemann S, Wirth R, Dresen G (2001) Synthesis of feldspar bicrystal by direct bonding. Phys Chem Miner 28: 685–692

Hill A, Wallach ER (1989) Modelling solid-state diffusion bonding. Acta Metal 37: 2425–2437

Hiraga T, Nagase T, Akizuki M (1999) The structure of grain boundaries in granite-origin ultramylonite studied by high-resolution electron microscopy. Phys Chem Miner 26: 617–623

Hutt S, Kienzle O, Ernst F, Rühle M (2000) Processing and structure of grain boundaries in strontium titanate. Z Metallk 92: 105–109

Lacroix A (1912) Note préliminaire sur quelques minéraux de Madagascar dont plusieurs peuvent tre utilisés comme gemmes. C R Acad Sci Paris 155: 672–677

Nyfeler D, Berger R, Gerber, C (1997) Scanning force microscopy on albite cleavage surfaces. Schweiz Mineral Petroc Mit 77: 21–26

Orhan N, Aksoy M, Eroglu M (1999) A new model for diffusion bonding and its application to duplex alloys. Mater Sci Eng (A)271: 458–468

Paulus H, Müller G (1988) The crystal structure of a hydrogen-feldspar. N Jb Miner Mh 11: 481–490

Pellegrini S (1971) A study of optimal twin boundaries. Ph. D. thesis Diss No: 4652, Swiss Federal Institute of Technology Zurich

Penn RL, Banfield JF (1998) Oriented attachment and growth, twinning, polytypism, and formation of metastable phases: insights from nanocrystalline TiO_2. Am Mineral 83: 1077–1082

Priess U (1981) Untersuchungen zur Tief-Hoch-Umwandlung von Fe-haltigen Orthoklas-Kristallen aus Madagaskar. N Jb Miner Abh 141: 17–29

Salje EKH (1990) Phase transitions in ferroelastic and co-elastic crystals. Cambridge University Press, Cambridge

Salje EKH (1995) Chemical mixing and structural phase transitions; the plateau effect and oscillatory zoning near surfaces and interfaces. Eur J Mineral 7: 791–806

Smith, JV (1988) Feldspar minerals. Springer, Berlin Heidelberg New York

Strecker A, Salzberger U, Mayer J (1993) Probenpräparation für die Transmissionselektronenmikroskopie: Verläßliche Methode für Querschnitte und brüchige Materialien. Prakt Metallogr 30: 482–489

Sutton AP, Balluffi RW (1995) Interfaces in crystalline materials. Monographs on the physics and chemistry of materials, vol 51. Clarendon Press, Oxford

Taylor WH, Darbyshire JA, Strunz H (1934) An X-ray investigation of the feldspars. Z Kristallogr 87: 464–498

Teng HH, Fenter P, Cheng L, Sturchio NC (2001) Resolving orthoclase dissolution processes with atomic force microscopy and X-ray reflectivity. Geochim Cosmochim Acta 65: 3459–3474

White JC, White SH (1981) On the structure of grain boundaries in tectonites. Tectonophysics 78: 613–628

Wolf D, Yip S (1992) Materials interfaces: atomic-level structure and properties. Chapman & Hall, London

Wooster WA (1981) Atomic arrangements on the twin boundaries of orthoclase twins. Mineral Mag 44: 351–353

Xu H, Buseck PR, Carpenter MA (1997) Twinning in synthetic anorthite: a transmission electron microscopy investigation. Am Mineral 82: 125–130

Zorz M, Follner H, Mirti B, Goli L (1998) Twin systematic of the monoclinic potassium feldspars as a result of their "Faden" growth in the alpine veins. N Jb Miner Abh 173: 1–22